JACS
JOURNAL OF THE AMERICAN CHEMICAL SOCIETY

ARTICLE

pubs.acs.org/JACS

# $^1$H NMR Chemical Shift Calculations as a Probe of Supramolecular Host−Guest Geometry

Jeffrey S. Mugridge, Robert G. Bergman,* and Kenneth N. Raymond*

Department of Chemistry, University of California, Berkeley and Chemical Science Division, Lawrence Berkeley National Laboratory, Berkeley, California 94720-1460, United States

Supporting Information

**ABSTRACT:** The self-assembled supramolecular host $[Ga_4L_6]^{12-}$ (**1**; $L$ = 1,5-bis[2,3-dihydroxybenzamido]naphthalene) can encapsulate cationic guest molecules within its hydrophobic cavity and catalyze the chemical transformations of bound guests. The cavity of host **1** is lined with aromatic naphthalene groups, which create a magnetically shielded interior environment, resulting in upfield shifted (1−3 ppm) NMR resonances for encapsulated guest molecules. Using gauge independent atomic orbital (GIAO) DFT computations, we show that $^1$H NMR chemical shifts for guests encapsulated in **1** can be efficiently and accurately calculated and that valuable structural information is obtained by comparing calculated and experimental chemical shifts. The $^1$H NMR chemical shift calculations are used to map the magnetic environment of the interior of **1**, discriminate between different host−guest geometries, and explain the unexpected downfield chemical shift observed for a particular guest molecule interacting with host **1**.

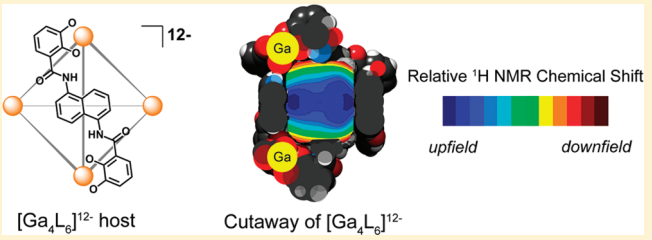


## INTRODUCTION

The NMR chemical shift is a remarkably sensitive and informative probe of nuclear chemical environment. The combination of density functional theory (DFT) based calculations with the gauge independent atomic orbital (GIAO) method for calculating nuclear shielding tensors has provided an accurate approach to calculating NMR chemical shifts in the solution and solid states.[1−3] Many researchers have successfully used DFT-based GIAO calculations to predict NMR chemical shifts and provide insight into a variety of experimental problems, typically involving molecular structure and/or conformation.[4−17] Recently, several groups have applied NMR chemical shift calculations to supramolecular host−guest complexes to investigate supramolecular self-assembly,[18] guest binding and molecular recognition,[19−23] as well as encapsulated guest conformation.[24] Supramolecular systems are typically well-suited to interrogation via NMR-based methods since guest encapsulation often dramatically changes the guest's electronic environment, resulting in pronounced chemical shift changes.[25] However, the large size of many supramolecular host−guest systems presents some computational challenges, since the DFT level of theory necessary to accurately predict chemical shifts becomes computationally very expensive with large atom numbers. Herein, we show that by treating a supramolecular host and its guest with differently sized basis sets, $^1$H NMR chemical shifts can be accurately and efficiently calculated, yielding valuable structural information.

The self-assembled supramolecular complex $[Ga_4L_6]^{12-}$ (**1**; Figure 1; $L$ = 1,5-bis[2,3-dihydroxybenzamido]naphthalene) can act as a host for suitably sized monocationic and neutral guest molecules.[26−30] Encapsulation within **1** has been shown to alter guest reactivity and catalyze a variety of chemical transformations, with accelerations as large as 2 million.[31−34] These large rate accelerations cannot be explained by only guest binding; they imply enzyme-like binding of the transition state. The singular interior space of host assembly **1** is dominated by the six naphthalene walls in the assembly framework. Due to the aromatic ring currents generated by these naphthalene groups, encapsulated guest molecules experience a magnetically shielded environment. The result is that the NMR resonances for guest molecules encapsulated within **1** are typically moved 1−3 ppm upfield from their NMR chemical shifts in bulk solution, provided that interior/exterior guest exchange is slow on the NMR time scale.[35] Such a large difference in the NMR chemical shift for free and encapsulated guests is useful both because it makes the observation of guest encapsulation simple and unambiguous and because it allows the behavior of interior and exterior guests to be monitored independently by NMR. This fortuitous separation in NMR chemical shifts has allowed for the measurement of many physical properties of supramolecular host **1**, such as the thermodynamics and kinetics of guest binding and exchange.[36−42]

The NMR chemical shifts of encapsulated guest molecules can in principle also provide structural information, such as the average orientation of a guest within the host cavity. Figure 2 shows the $^1$H NMR spectra of two host−guest complexes; for each, the encapsulated guest $^1$H NMR resonances are distinct and well-separated, suggesting different average positions and

**Received:** March 11, 2011
**Published:** June 29, 2011

  

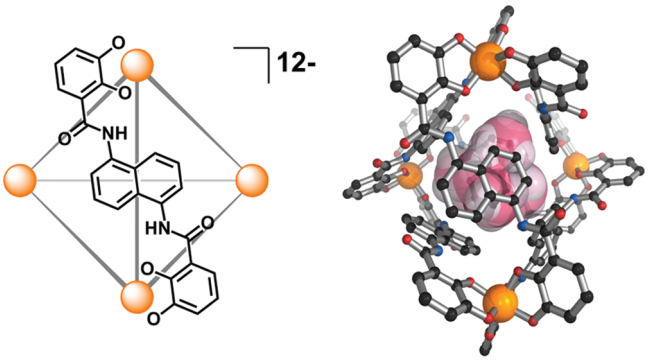


**Figure 1.** (Left) Schematic illustration of supramolecular host **1** with only one ligand shown for clarity. (Right) Model of the host–guest complex $[NEt_4 \subset \mathbf{1}]^{11-}$, where $\subset$ denotes encapsulation.

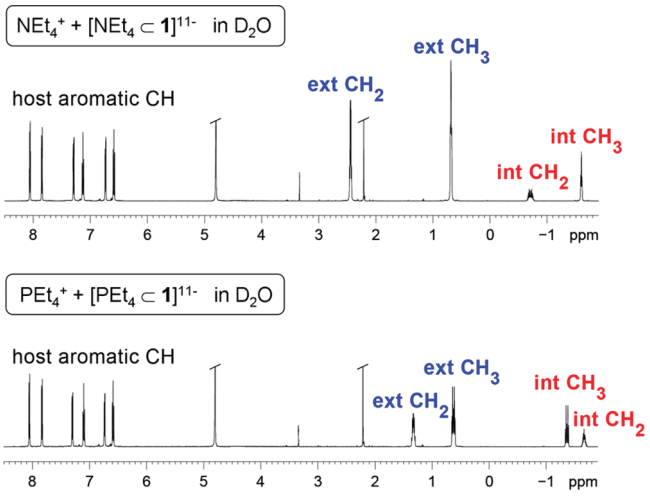


**Figure 2.** $^1$H NMR spectra of $NEt_4^+$ + **1** (top) and $PEt_4^+$ + **1** (bottom) in $D_2O$. Encapsulated/interior (red int) and unencapsulated/exterior (blue ext) guest resonances are labeled.

**Chart 1**

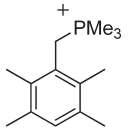


**2**

chemical environments for the various protons (i.e., $CH_3$, $CH_2$) of each guest molecule. Although these guests tumble rapidly on the NMR time scale inside of **1** and the observed chemical shifts are the time-average of many guest orientations, knowledge of the magnetic environment of the host interior can provide information about the low-energy guest conformations and orientations within the host cavity. Solution-state structural information is especially valuable for supramolecular host **1**, since crystallization of these host–guest complexes is problematic.

Further motivation to investigate the NMR chemical shifts of encapsulated guest molecules computationally comes from the

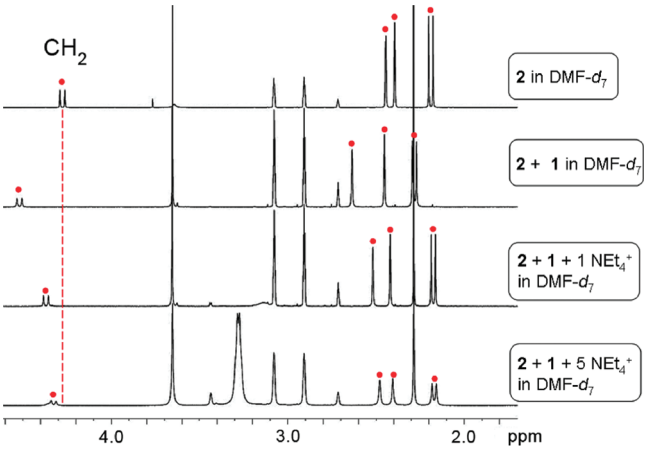


**Figure 3.** $^1$H NMR spectra showing the downfield shift of the proton resonances of guest **2** (red ●) upon interaction with host **1** in DMF-$d_7$. (Top) **2** in bulk DMF-$d_7$; (2nd from top) $^1$H NMR resonances of **2** shift downfield by ~0.2 ppm upon addition of **1**; (bottom) addition of $NEt_4^+$ to block the host cavity and exterior binding sites results in the resonances of **2** moving upfield toward their positions in bulk DMF-$d_7$.

observation of surprising NMR chemical shifts for some host–guest complexes. For example, closer inspection of the encapsulated guest region in the $^1$H NMR spectra for $[NEt_4 \subset \mathbf{1}]^{11-}$ and $[PEt_4 \subset \mathbf{1}]^{11-}$ (Figure 2) reveals that for $NEt_4^+$, the $CH_3$ resonance is *upfield* of the $CH_2$ resonance, whereas the reverse is true for $PEt_4^+$.[43] Even more curious, the interaction of guest **2** (Chart 1) with host **1** in DMF-$d_7$ results in a *downfield* shift relative to that guest's NMR chemical shift in bulk solution (Figure 3).[44] This is the first downfield shift that has been observed for a guest interacting with **1**, for either interior or exterior host binding.

This work describes the application of DFT-based GIAO NMR chemical shift calculations to guest molecules encapsulated in supramolecular host **1**. It is found that despite the large size of these systems (~300 atoms), by treating host and guest with small and large basis sets, respectively, $^1$H NMR chemical shifts for the encapsulated guest can be efficiently and accurately calculated. This methodology is then applied to the dynamic process of guest exchange, which suggests an explanation for the unexpected downfield shift of **2** described above. In combination with in situ NMR spectroscopy, these NMR chemical shift calculations provide a useful probe of solution-state host–guest geometry.

## RESULTS AND DISCUSSION

**Calculated $^1$H NMR Chemical Shifts of a Hypothetical Methane Guest.** The magnetic environment of the host cavity was first investigated by calculating the relative $^1$H NMR chemical shift changes on the interior of **1**. For these calculations, the host geometry from the solid-state structure of $[Cp^*_2Co \subset \mathbf{1}]^{11-}$ was used[30] and a molecule of methane was incrementally moved along two paths spanning the host interior: from vertex to aperture and from naphthalene wall to naphthalene wall (Figure 4, a). The $^1$H NMR chemical shift of the methane probe was then calculated at different points along each path (Figure 4, b). The calculated $^1$H NMR chemical shifts of the four individual protons of methane were not the same and typically differed by ~0.2 ppm, but in a few cases differed by more than 2 ppm; the individual


dx.doi.org/10.1021/ja202254x |J. Am. Chem. Soc. 2011, 133, 11205–11212

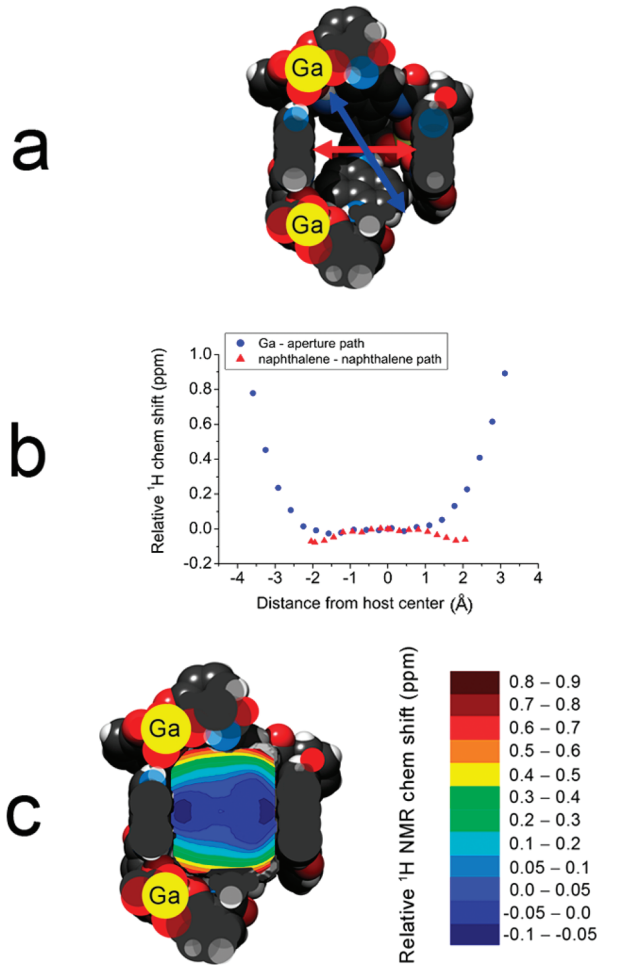


**Figure 4.** (a) Cutaway of host **1** showing the paths along which $^1$H NMR chemical shifts for methane were calculated. (b) Plot of the average $^1$H NMR chemical shift for methane at various distances from the host center along the paths shown in a; the average chemical shift of methane at the host center is set to zero. (c) Cutaway of host **1** showing a contour map of the change in average $^1$H NMR chemical shift of methane, relative to the host center. The contour map was generated in OriginPro 8.1[47] from the data shown in b and the application of host symmetry.

calculated shifts were averaged to give the average $^1$H NMR chemical shift for methane. The GIAO NMR shift calculations were carried out in Gaussian 09[45] in a water dielectric and host atoms were treated with B3LYP/3-21 g while guest atoms were treated with B3LYP/6-311 g(d,p). The lower level of theory applied to the host is sufficient to model electronic shielding effects felt by the encapsulated guest while keeping computational cost reasonable, but it is insufficient to provide accurate NMR chemical shifts for host protons and these were generally observed to differ from experimental values by 1−4 ppm.[46] By applying the host symmetry (the naphthalene−naphthalene path is along a 2-fold rotational axis) to the calculated chemical shift data, a spatial map of the relative changes in guest chemical shift on the interior of **1** can be generated (Figure 4, c).

As methane is moved from the host center toward either a metal vertex, or in the opposite direction toward an aperture, its calculated average $^1$H NMR chemical shift increases by nearly 1 ppm relative to the center of the host. In contrast, moving methane from the host center toward any of the naphthalene walls results in almost no change in the average chemical shift: a decrease of less than 0.1 ppm is observed relative to the host center. Assuming that this hypothetical methane probe provides a good approximation of the local magnetic environment experienced by guest moieties, it would be expected that, for example, the $^1$H NMR resonances of encapsulated methyl groups positioned near the host apertures or vertices would be significantly downfield-shifted relative to those positioned close to the naphthalene walls.

**Table 1. Calculated and Experimental $^1$H NMR Chemical Shifts and the Calculated Void Space Cavity Volumes ($V$; from Voidoo[51,52]) for Various Host-Guest Complexes[a]**

| | | $^1$H NMR chemical shift (ppm), obtained from the following: | | |
|---|---|---|---|---|
| host−guest complex | moiety | solid-state[b] | CS, MM minimization[c] | experimental[d] |
| [**NEt$_4$** ⊂ **1**]$^{11-}$ | $NCH_2CH_3$ | −1.22 | −1.53 | −1.53 |
| | $NCH_2CH_3$ | −0.84 | −0.71 | −0.61 |
| | | ($V$ = 268 Å$^3$) | ($V$ = 392 Å$^3$) | |
| [**PEt$_4$** ⊂ **1**]$^{11-}$ | $NCH_2CH_3$ | | −1.30 | −1.31 |
| | $NCH_2CH_3$ | | −1.58 | −1.60 |
| | | | ($V$ = 414 Å$^3$) | |
| [**NMe$_3$Bn** ⊂ **1**]$^{11-}$ | $NCH_3$ | −0.10 | 0.67 | −0.15 |
| | $NCH_2$ | 0.15 | 1.09 | 0.75 |
| | ArH | 4.87 (*o*) | 4.63 (*o*) | 4.13 (*o*) |
| | | 5.46 (*m*) | 6.00 (*m*) | 5.33 (*m*) |
| | | 5.19 (*p*) | 5.51 (*p*) | 6.02 (*p*) |
| | | ($V$ = 300 Å$^3$) | ($V$ = 450 Å$^3$) | |
| [**3** ⊂ **1**]$^{11-}$ | $PCH_3$ | −0.91 | −0.84 | −0.97 |
| | $PCH_2$ | 0.13 | 0.31 | −0.04 |
| | $ArCH_3$ | 0.50, 0.55 (*o*) | 0.44, 0.45 (*o*) | 0.43, 0.50 (*o*) |
| | | 0.37 (*p*) | 0.78 (*p*) | 0.65 (*p*) |
| | ArH | 3.54, 4.91 | 5.01, 5.26 | 3.69, 4.57 |
| | | ($V$ = 367 Å$^3$) | ($V$ = 435 Å$^3$) | |

[a] For all NMR shift calculations, host atoms were treated with B3LYP/3-21g and guest atoms with B3LYP/6-311g(d,p) in a continuous water dielectric. [b] Host−guest geometries obtained from solid-state structures,[30] with minimization (OPLS 2005) of the guest only to correct for C−H bond lengths underestimated by the diffraction experiment.[48] [c] Host−guest geometries obtained from conformational searching and minimization (OPLS 2005) of both host and guest. [d] Experimental $^1$H NMR chemical shifts were measured in $D_2O$ ($\delta$ = 4.80) at 500 MHz and 298 K with [**1**] = 1 mM and 0.9 equivalents guest. *o*, *m*, and *p*, refer to ortho, meta, and para aromatic protons, respectively.

**Calculated versus Experimental $^1$H NMR Chemical Shifts.** The relative $^1$H NMR chemical shifts calculated using a methane probe may give qualitative information about how a guest is oriented within the host cavity, but because methane is only a hypothetical guest (it has never been observed experimentally inside of **1**) these calculations cannot be compared directly to experimental NMR spectroscopy data. To investigate whether the GIAO computational method can predict $^1$H NMR chemical shifts for guests encapsulated in **1** that accurately match those obtained experimentally, the shifts for several known host−guest complexes were calculated (Table 1). The host−guest geometries for these calculations were obtained in one of two ways: (a) from

solid-state structure coordinates,[48] or (b) from molecular mechanics-based conformational searching (MacroModel,[49] OPLS 2005[50]), in which the host and guest geometries were subjected to Monte Carlo conformational searching and minimized using molecular mechanics. These host−guest geometries were then submitted for DFT-level GIAO calculations (note that there is no minimization in this step) with the same basis sets and conditions described above for the encapsulated methane calculations. The calculated $^1$H NMR chemical shifts of protons that are chemically equivalent in solution (e.g., $CH_3$ protons of a methyl group, which are related via rapid bond rotation) were averaged.

For the simple guests $NEt_4^+$ and $PEt_4^+$, the agreement between the calculated and experimental $^1$H NMR chemical shifts is excellent. The GIAO computations nicely predict the reversal of the $CH_2$ and $CH_3$ resonances for encapsulated $NEt_4^+$ ($CH_3$ upfield of $CH_2$) versus $PEt_4^+$ ($CH_2$ upfield of $CH_3$) observed in solution. For the aromatic guests $NMe_3Bn^+$ and **3** (Chart 2), agreement between experimental and calculated chemical shifts is not nearly as striking, but still quite good. Comparing the calculated chemical shifts for solid-state versus minimization-derived host−guest geometries, neither is significantly more accurate than the other, suggesting that the magnetic environment of the interior is relatively independent of host cavity volume ($V$ in Table 1; which is consistently ~150 Å$^3$ larger for mechanics-minimized geometries[53]).

It is not surprising that GIAO calculations with the higher symmetry guests $NEt_4^+$ and $PEt_4^+$ show better agreement with experiment than the lower symmetry benzyl phosphonium/ammonium guests: the experimental $^1$H NMR chemical shifts measured in solution are actually an average of many different host−guest orientations and conformations (the guest tumbles rapidly on the NMR time scale inside the host cavity), while the calculated chemical shifts are taken from one static host−guest geometry. For calculations with the tetrahedrally symmetric $NEt_4^+$ and $PEt_4^+$, a single host−guest geometry is sufficient because the four ethyl groups effectively sample the different conformations and magnetic environments experienced by a rapidly tumbling guest in solution. However, this is not necessarily true for the aromatic guests, where a different orientation within the cavity would produce markedly different chemical shifts (see below). Calculating the $^1$H NMR chemical shifts for each aromatic guest in many different orientations within the host, then averaging those shifts, may lead to improved agreement between computation and experiment.

If the GIAO calculations described above are to be useful in helping decode solution-state host−guest structure, then they must be able to discriminate between different encapsulated guest orientations. From the encapsulated methane calculations, it is not immediately obvious that this discrimination is possible, since the symmetry of the assembly and the similarity of the magnetic environment near the apertures and vertices would suggest that many guest orientations might have indistinguishable chemical shifts. To address this possibility, the $^1$H NMR chemical shifts of alternate host−guest geometries for $[PEt_4^+ \subset \mathbf{1}]^{11-}$ and $[NMe_3Bn^+ \subset \mathbf{1}]^{11-}$ generated from the conformational searches were calculated (CS, MM minimization 2; Table 2). The alternative host−guest geometries have $PEt_4^+$ off-center in the host cavity (the original minimization-derived structure has the guest centered in the host cavity), and the aromatic meta and para C−H bonds of $NMe_3Bn^+$ point toward a host vertex (the original minimization-derived geometry has those aromatic C−H bonds pointing toward a host aperture; Figure 5).

For both $PEt_4^+$ and $NMe_3Bn^+$, GIAO calculations with the two different host−guest geometries taken from their respective conformational searches yield noticeably different $^1$H NMR

**Chart 2**

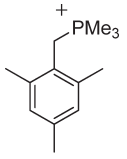


**3**

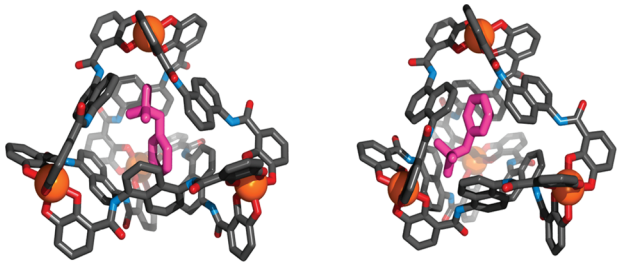

**Figure 5.** "CS, MM minimization" (left) and "CS, MM minimization 2" (right) host−guest geometries for $[NMe_3Bn^+ \subset \mathbf{1}]^{11-}$. As shown in Table 2, these different geometries give different calculated $^1$H NMR chemical shifts.

**Table 2. Calculated and Experimental $^1$H NMR Chemical Shifts for Various Host-Guest Complexes and Guest Orientations**

| | | $^1$H NMR chemical shift (ppm), obtained from the following: | | |
|---|---|---|---|---|
| host−guest complex | moiety | CS, MM minimization[a] | CS, MM minimization 2[b] | experimental[c] |
| $[\mathbf{PEt_4} \subset \mathbf{1}]^{11-}$ | $NCH_2CH_3$ | −1.30 | −1.45 | −1.31 |
| | $NCH_2CH_3$ | −1.58 | −1.47 | −1.60 |
| $[\mathbf{NMe_3Bn} \subset \mathbf{1}]^{11-}$ | $NCH_3$ | 0.67 | 1.09 | −0.15 |
| | $NCH_2$ | 1.09 | 1.05 | 0.75 |
| | ArH | 4.63 (*o*) | 4.57 (*o*) | 4.13 (*o*) |
| | | 6.00 (*m*) | 6.00 (*m*) | 5.33 (*m*) |
| | | 5.51 (*p*) | 7.71 (*p*) | 6.02 (*p*) |

[a] Host−guest geometries obtained from conformational searching and minimization (OPLS 2005) of both host and guest, repeated from Table 1. [b] Alternate host−guest geometries (different from CS, MM minimization) selected from conformational searching and minimization (OPLS 2005) of both host and guest. [c] Experimental $^1$H NMR chemical shifts, see Table 1 for conditions.

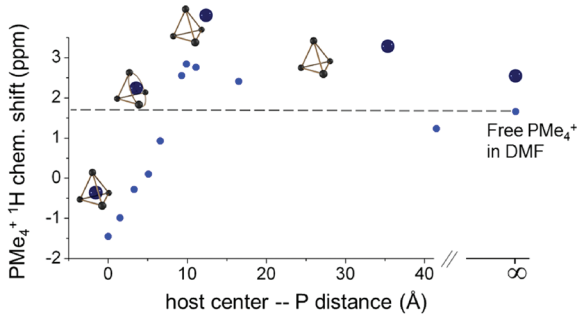


**Figure 6.** Plot of the calculated, average $^1$H NMR chemical shifts of $PMe_4^+$ during guest ejection from host **1** in a DMF dielectric.[44] Ball and stick schematics illustrate the approximate host−guest distances and geometries along the exchange pathway. The dotted line marks the $^1$H NMR chemical shift of $PMe_4^+$ calculated in a DMF dielectric in the absence of **1**.

chemical shifts. Shifts calculated for the CS, MM minimization 2 geometries ($PEt_4^+$ off-center, $NMe_3Bn^+$ oriented with its para C−H pointed toward a host vertex) show worse agreement with experiment than those for the CS, MM minimization geometries ($PEt_4^+$ centered, $NMe_3Bn^+$ oriented with its para C−H pointed toward a host aperture), suggesting that the latter orientations are closer to the solution-state, average host−guest geometries. Despite the tetrahedral symmetry of host **1** and the high degree of redundancy in the magnetic environment of the interior cavity, DFT-based GIAO NMR shift calculations are able not only to accurately predict experimental $^1$H NMR chemical shifts, but also to distinguish between different host−guest geometries. These calculations provide some insight into the solution-state structure and orientation of guest molecules encapsulated within **1**.

**Calculated $^1$H NMR Chemical Shifts During Guest Exchange.** Having successfully mapped the magnetic environment for the interior cavity of **1** and shown that experimental $^1$H NMR chemical shifts can be accurately predicted with GIAO NMR shift calculations, this methodology was next applied to the guest exchange process, in order to address the curious observation of downfield shifted guest resonances for **2**. 2D $^1$H−$^1$H EXSY NMR experiments show that guest **2** enters and exits host **1** rapidly on the NMR time scale in DMF-$d_7$ solution (see Supporting Information). The hypothesis is that while **2** exchanges quickly, on average, it sits near one of the apertures on the outside of host **1** and this position, which is in-plane with three naphthalene rings, is magnetically deshielded and responsible for the observed downfield shift of the guest NMR resonances relative to their frequencies in bulk solution. To test whether the space near the host apertures is sufficiently magnetically deshielding to shift guest resonances downfield, $^1$H NMR chemical shifts for the simple guest $PMe_4^+$ were calculated at various points along its guest ejection pathway (Figure 6). Host−guest geometries during the guest ejection process were calculated using molecular mechanics minimizations (CAChe 6.1, MM3) as previously described.[41]

As $PMe_4^+$ moves from the center of **1** toward an aperture on the interior of the host, its average $^1$H NMR chemical shift moves progressively downfield, consistent with the methane-based calculations discussed above. As it passes through the aperture and onto the host exterior, the guest chemical shifts initially continue to move downfield and as the guest moves further and further away from the host, its chemical shifts tend upfield toward their position in bulk solution. These calculations predict that the space on the exterior of **1** near the host apertures is significantly deshielded and that the $^1$H NMR resonances of $PMe_4^+$ are shifted nearly 1 ppm downfield from their position in bulk DMF. This suggests that guest **2** might sit near the host apertures in DMF solution and quickly exchange into and out of **1**, such that on average its $^1$H NMR chemical shifts are moved downfield relative to their position in bulk DMF. In the solid-state host−guest structures with **3**[54] and $NMe_3Bn^+$,[30] both have guest molecules bound to the exterior of the host that sit very close to one of the apertures; it is therefore reasonable to assume that the structurally similar **2** can bind in this manner as well, lending further support to the above explanation of its downfield-shifted NMR resonances.

## CONCLUSIONS

DFT-based GIAO NMR chemical shift calculations in conjunction with in situ NMR spectroscopy provide a powerful tool for investigating solution-state molecular structure. Although supramolecular host−guest systems with **1** are very large and thus present some computational challenges at the DFT level of theory, by applying a smaller basis set to the host and a much larger basis set to the guest, NMR chemical shifts for the encapsulated guest can be predicted both efficiently and accurately. The interior and exterior magnetic environment of host **1** was investigated through GIAO calculations in several ways: (1) a qualitative, spatial map of the magnetic shielding felt by encapsulated guests was generated using methane to probe the relative changes in $^1$H NMR chemical shifts at different locations on the host interior; (2) the $^1$H NMR chemical shifts for host−guest complexes in several orientations and geometries were predicted computationally and compared with solution-state NMR experiments; and (3) the computational method was applied to the dynamic process of guest exchange to help explain the unexpected downfield shifting of a particular guest's NMR resonances.

The calculated $^1$H NMR chemical shifts for encapsulated guests accurately reproduce those obtained experimentally, and for all three cases described above, the GIAO calculations provide information about solution-state host−guest geometry. While the magnetic environment of the host interior is not sufficiently diverse to predict specific host−guest geometries from a simple $^1$H NMR spectrum (due to host symmetry and similarities in local shielding), the combination of computational and experimental NMR chemical shifts can provide information about the average guest orientation and/or conformation within host **1**. The DFT-based GIAO NMR shift calculations described here are a first step in elucidating how the conformations and orientations of encapsulated guests affect host-mediated reactivity and catalysis in solution. We expect that this computational approach can also be applied by other researchers to accurately and efficiently calculate NMR chemical shifts for a variety of large, supramolecular host−guest systems and provide valuable solution-state structural information.

## EXPERIMENTAL SECTION

**General.** Unless otherwise noted, manipulations were carried out using standard Schlenk and high-vacuum techniques and all chemicals were obtained from commercial suppliers and used without further purification. All glassware was oven-dried at 150 °C. All solvents were sparged with nitrogen prior to use. The preparation and characterization

of host−guest complexes with $NEt_4^+$, $PEt_4^+$, $NMe_3Bn^+$, and **3** have been previously reported.[25,26,29,50]

**Procedures for NMR Spectroscopy.** Host−guest complex solutions were prepared under nitrogen in degassed solvent by mixing stock solutions of host and guest in $D_2O$ and filtered through 0.2 $\mu$m syringe filters prior to use. The final concentrations of the host−guest solutions analyzed by NMR had [**1**] = 1 mM and [guest] = 0.9 mM; the slight excess of host ensures nearly quantitative encapsulation of guest and no perturbations on encapsulated guest chemical shifts due to exterior guest association. All $^1$H NMR spectra were acquired on a Bruker AV-500 NMR spectrometer at 298 K and the chemical shifts were referenced relative to residual protic solvent resonances ($\delta$ 4.80 for $D_2O$ and $\delta$ 2.75 for DMF-$d_7$).

**Computational Methods.** All DFT calculations were carried out in the UC Berkeley Molecular Graphics and Computation Facility using Gaussian 09 software with GaussView graphical user interface.[45] For all GIAO $^1$H NMR chemical shift calculations, all host atoms were treated with B3LYP/3-21 g and all guest atoms were treated with B3LYP/6-311 g(d,p). The calculated guest $^1$H NMR chemical shifts were referenced to those calculated for trimethylsilane at the B3LYP/6-311 g(d,p) level of theory. All GIAO calculations were carried out with a continuous dielectric solvent model (either water or DMF).

For the encapsulated methane calculations, methane was systematically moved across the host interior as described in the Results and Discussion section and the methane molecule was stopped just before the van der Waals radii of host and guest came into contact. The $^1$H NMR chemical shifts of methane were calculated at each point and the chemical shifts for each of methane's four protons were averaged. For the host−guest structure calculations, the calculated $^1$H NMR chemical shifts for those protons which are expected to be chemically equivalent in solution were averaged; for example, all nine protons for the methyl groups in $NMe_3Bn^+$ were averaged because rapid bond rotation in solution will make these equivalent by NMR. For the same reasons, in the $PMe_4^+$ guest exchange calculations all methyl protons were averaged. The calculated $^1$H NMR chemical shifts for individual protons that are expected to be chemically equivalent in solution typically differed by up to ∼0.3 ppm, but in some cases these differed by greater than ∼2 ppm.

**2,3,5,6-Tetramethylbenzyl Alcohol.** 2,3,5,6-Tetramethylbenzoic acid (2.0 g, 11.0 mmol, 1 equivalent) was dissolved in THF and added dropwise to a cooled (−30 °C) suspension of lithium aluminum hydride (LAH; 851 mg, 22.0 mmol, 2 equivalents) in THF under $N_2$. The suspension was warmed to room temperature and refluxed for 20 h. The LAH suspension was then cooled to 0 °C and a saturated, aqueous solution of sodium sulfate was slowly added dropwise under $N_2$. This reaction is very exothermic and care must be taken to not quench the LAH too quickly. Once the LAH suspension was quenched and visibly stopped reacting with the added water, the solution was filtered and the layers of the filtrate were separated. TLC of the organic layer showed a mixture of product and starting material, so the crude product mixture was redissolved in THF and added to a fresh suspension of LAH (1.27 g, 34 mmol, 3 equiv). The suspension was refluxed for 2 days under $N_2$. After quenching and separating organic and aqueous phases as above, the aqueous layer was washed with diethyl ether (3 × 100 mL) and the organic layers were combined and dried with $MgSO_4$. The ether was removed under reduced pressure to give a white solid with yield 513 mg (27%). $^1$H NMR (400 MHz, $CDCl_3$): $\delta$ 6.94 (s, 1H, ArH), 4.77 (d, $J$ = 4.4 Hz, 2H, benzyl $CH_2$), 2.29 (s, 6H, $ArCH_3$), 2.23 (s, 6H, $ArCH_3$), 1.21 (br, 1H, OH). $^{13}$C{$^1$H} NMR (100 MHz, $CDCl_3$): $\delta$ 136.5 (ArC), 134.2 (ArC), 133.3 (ArC), 131.7 (ArC), 59.8 (benzyl $CH_2$), 20.4 ($ArCH_3$), 15.2 ($ArCH_3$).

**2,3,5,6-Tetramethylbenzyl Bromide.** 2,3,5,6-Tetramethylbenzyl alcohol (0.5 g, 3.0 mmol, 1.0 equiv) was dissolved in diethyl ether in a warm, oven-dried Schlenk flask. The solution was sparged with $N_2$ and cooled to −78 °C in a $CO_2$/acetone cold bath. $PBr_3$ (0.35 mL, 3.7 mmol, 1.2 equiv) was added directly to the ether solution via syringe and the reaction mixture was allowed to slowly warm to room temperature and stirred overnight. The resulting light orange solution was poured over ice to quench any remaining $PBr_3$ and the layers were separated. The aqueous layer was extracted with diethyl ether (2 × 100 mL) and the organic layers are combined, washed with saturated aqueous bicarbonate and then dried over $MgSO_4$. The ether solvent was removed by rotary evaporation to give a white solid with yield 400 mg (58%). $^1$H NMR (400 MHz, $CDCl_3$): $\delta$ 6.97 (s, 1H, ArH), 4.64 (s, 2H, benzyl $CH_2$), 2.31 (s, 6H, $ArCH_3$), 2.26 (s, 6H, $ArCH_3$). $^{13}$C{$^1$H} NMR (100 MHz, $CDCl_3$): $\delta$ 134.1 (ArC), 134.0 (ArC), 133.5 (ArC), 132.0 (ArC), 30.8 (benzyl $CH_2$), 20.4 ($ArCH_3$), 15.0 ($ArCH_3$).

**2,3,5,6-Tetramethylbenzyltrimethyl Phosphonium Bromide (2[Br]).** 2,3,5,6-Tetramethylbenzyl bromide (370 mg, 1.6 mmol, 1 equiv) was dissolved in diethyl ether (75 mL) and sparged with $N_2$ for 10 min. Trimethyl phosphine (0.42 mL, 4.1 mmol, 2.5 equiv) was added to the reaction flask via syringe. The solution was stirred overnight under nitrogen atmosphere and the resulting white precipitate was collected by vacuum filtration and washed with diethyl ether (3 × 30 mL). After removing residual solvent overnight under high vacuum, the product was obtained as a white solid with yield 400 mg (82%). $^1$H NMR (500 MHz, $CD_3OD$): $\delta$ 6.96 (s, 1H, ArH), 3.90 (d, $J$ = 16.5 Hz, 2H, benzyl $CH_2$), 2.20 (br, 12H, $ArCH_3$), 1.81 (d, $J$ = 14.4 Hz, 9H, $PMe_3$). $^{13}$C{$^1$H} NMR (125 MHz, $CD_3OD$): $\delta$ 135.1 (d, $J$ = 4.2 Hz, ArC), 133.0 (d, $J$ = 5.5 Hz, ArC), 131.3 (d, $J$ = 4.2 Hz, ArC), 125.1 (d, $J$ = 9.3 Hz, ArC), 24.4 (d, $J$ = 50.0 Hz, benzyl $CH_2$), 19.3 (s, $ArCH_3$), 16.3 (d, $J$ = 1.6 Hz, $ArCH_3$), 7.4 (d, $J$ = 53.8 Hz, $PMe_3$). $^{31}$P{$^1$H} NMR (202 MHz, $CD_3OD$): $\delta$ 28.4 (s). (ESIHR) for $C_{14}H_{24}P$, calcd (found) $m/z$: 223.1610 (223.1609).

**$K_{11}$[2 ⊂ 1].** The title host−guest complex was prepared in situ by mixing host $K_{11}$[**1**] with **2**[Br] in $D_2O$ under a nitrogen atmosphere. $^1$H NMR (600 MHz, $D_2O$): $\delta$ 8.13 (d, $J_{HH}$ = 7.8 Hz, 12H, *host* ArH), 7.65 (d, $J_{HH}$ = 8.4 Hz, 12H, *host* ArH), 7.35 (d, $J_{HH}$ = 7.8 Hz, 12H, *host* ArH), 6.91 (t, $J_{HH}$ = 8.4 Hz, 12H, *host* ArH), 6.75 (d, $J_{HH}$ = 7.8 Hz, 12H, *host* ArH), 6.61 (t, $J_{HH}$ = 7.8 Hz, 12H, *host* ArH), 4.20 (s, 1H, *encaps* ArH), 0.41 (m, 1H, *encaps* benzyl CH), 0.38 (s, 3H, *encaps* $ArCH_3$), 0.04 (m, 1H, *encaps* benzyl CH), −0.55 (s, 3H, *encaps* $ArCH_3$), −0.88 (d, $J_{PH}$ = 13.2 Hz, 9H, *encaps* $PMe_3$), −1.12 (s, 3H, *encaps* $ArCH_3$). HRMS (ESI−QTOF): calcd (found) $m/z$: $[\mathbf{1} + \mathbf{2} + 8K^+]^{3-}$ 1124.3633 (1124.3726), $[\mathbf{1} + \mathbf{2} + 7K^+ + H^+]^{3-}$ 1111.7113 (1111.7078), $[\mathbf{1} + \mathbf{2} + 7K^+]^{4-}$ 833.5317 (833.5209), $[\mathbf{1} + \mathbf{2} + 6K^+ + H^+]^{4-}$ 824.0428 (824.0475), $[\mathbf{1} + \mathbf{2} + 5K^+ + 2H^+]^{4-}$ 814.5538 (814.5443), $[\mathbf{1} + \mathbf{2} + 4K^+ + 2H^+]^{5-}$ 643.6506 (643.6408).

## ■ ASSOCIATED CONTENT

**Supporting Information.** 2D EXSY NMR spectrum of guest **2**, atom coordinates used for all GIAO NMR shift calculations. This material is available free of charge via the Internet at http://pubs.acs.org.

## ■ AUTHOR INFORMATION

**Corresponding Author**
rbergman@berkeley.edu; raymond@socrates.berkeley.edu

## ■ ACKNOWLEDGMENT

The authors would like to thank Dr. Jamin Krinsky and Dr. Kathleen Durkin for assistance with computational and modeling studies and acknowledge NSF Grants CHE-0233882 and CHE-0840505, which fund the UC Berkeley Molecular Graphics and Computational Facility. This work has been supported by the Director, Office of Science, Office of Basic Energy Sciences, Division of Chemical Sciences, Geosciences, and Biosciences

of the U.S. Department of Energy at LBNL under Contract No. DE-AC02-05CH11231 and an NSF predoctoral fellowship to J.S.M.

## REFERENCES


(1) Ditchfield, R. *Mol. Phys.* **1974**, *27*, 789–807.
(2) Wolinski, K.; Hinton, J. F.; Pulay, P. *J. Am. Chem. Soc.* **1990**, *112*, 8251–8260.
(3) Cheeseman, J. R.; Trucks, G. W.; Keith, T. A.; Frisch, M. J. *J. Chem. Phys.* **1996**, *104*, 5497–5509.
(4) Smith, S. G.; Goodman, J. M. *J. Am. Chem. Soc.* **2010**, *132*, 12946–12959.
(5) Onak, T.; Tran, D.; Tseng, J.; Diaz, M.; Arias, J.; Herrera, S. *J. Am. Chem. Soc.* **1993**, *115*, 9210–9215.
(6) Barfield, M.; Fagerness, P. *J. Am. Chem. Soc.* **1997**, *119*, 8699–8711.
(7) Forsyth, D. A.; Sebag, A. B. *J. Am. Chem. Soc.* **1997**, *119*, 9483–9494.
(8) Meier, M. S.; Spielmann, H. P.; Bergosh, R. G.; Haddon, R. C. *J. Am. Chem. Soc.* **2002**, *124*, 8090–8094.
(9) Olah, G. A.; Surya Prakash, G. K.; Rasul, G. *J. Am. Chem. Soc.* **2008**, *130*, 9168–9172.
(10) Patel, D. G.; Paquette, M. M.; Kopelman, R. A.; Kaminsky, W.; Ferguson, M. J.; Frank, N. L. *J. Am. Chem. Soc.* **2010**, *132*, 12568–12586.
(11) Shoji, Y.; Matsuo, T.; Hashizume, D.; Fueno, H.; Tanaka, K.; Tamao, K. *J. Am. Chem. Soc.* **2010**, *132*, 8258–8260.
(12) Rasul, G.; Chen, J. L.; Prakash, G. K. S.; Olah, G. A. *J. Phys. Chem. A* **2010**, *114*, 4394–4399.
(13) Bal, D.; Kraska-Dziadecka, A.; Gryff-Keller, A. *J. Org. Chem.* **2009**, *74*, 8604–8609.
(14) Smith, S. G.; Goodman, J. M. *J. Org. Chem.* **2009**, *74*, 4597–4607.
(15) Okazaki, T.; Laali, K. K. *J. Org. Chem.* **2004**, *69*, 510–516.
(16) Gomila, R. M.; Quiñonero, D.; Rotger, C.; Garau, C.; Frontera, A.; Ballester, P.; Costa, A.; Deyà, P. M. *Org. Lett.* **2002**, *4*, 399–401.
(17) Sebag, A. B.; Forsyth, D. A.; Plante, M. A. *J. Org. Chem.* **2001**, *66*, 7967–7973.
(18) Ferrer, M.; Mounir, M.; Rossell, O.; Ruiz, E.; Maestro, M. A. *Inorg. Chem.* **2003**, *42*, 5890–5899.
(19) Chelli, S.; Majdoub, M.; Jouini, M.; Aeiyach, S.; Maurel, F.; Chane-Ching, K.; Lacaze, P. *J. Phys. Org. Chem.* **2007**, *20*, 30–43.
(20) Schatz, J.; Backes, A.; Siehl, H. *J. Chem. Soc., Perkin Trans. 2* **2000**, *4*, 609–610.
(21) Backes, A. C.; Schatz, J.; Siehl, H.-U. *J. Chem. Soc., Perkin Trans. 2* **2002**, 484–488.
(22) Buschmann, H.; Wego, A.; Zielesny, A.; Schollmeyer, E. *J. Inclusion Phenom. Macrocyclic Chem.* **2006**, *54*, 241–246.
(23) Klärner, F.-G.; Kahlert, B.; Nellesen, A.; Zienau, J.; Ochsenfeld, C.; Schrader, T. *J. Am. Chem. Soc.* **2006**, *128*, 4831–4841.
(24) Ajami, D.; Iwasawa, T.; Rebek, J. *Proc. Natl. Acad. Sci. U.S.A.* **2006**, *103*, 8934–8936.
(25) For recent examples, see:(a) Mal, P.; Breiner, B.; Rissanen, K.; Nitschke, J. R. *Science* **2009**, *324*, 1697–1699. (b) Hatakeyama, Y.; Sawada, T.; Kawano, M.; Fujita, M. *Angew. Chem., Int. Ed.* **2009**, *48*, 8695–8698. (c) Durola, F.; Rebek, J., Jr. *Angew. Chem., Int. Ed.* **2010**, *49*, 3189–3191. (d) Pluth, M. D.; Fiedler, D.; Mugridge, J. S.; Bergman, R. G.; Raymond, K. N. *Proc. Natl. Acad. Sci. U.S.A.* **2009**, *106*, 10438–10443. (e) Ferrand, Y.; Kendhale, A. M.; Kauffmann, B.; Grélard, A.; Marie, C.; Blot, V.; Pipelier, M.; Dubreuil, D.; Huc, I. *J. Am. Chem. Soc.* **2010**, *132*, 7858–7859. (f) Shoji, Y.; Matsuo, T.; Hashizume, D.; Fueno, H.; Tanaka, K.; Tamao, K. *J. Am. Chem. Soc.* **2010**, *132*, 8258–8260.
(26) Caulder, D. L.; Powers, R. E.; Parac, T. N.; Raymond, K. N. *Angew. Chem., Int. Ed.* **1998**, *37*, 1840–1843.
(27) Parac, T. N.; Caulder, D. L.; Raymond, K. N. *J. Am. Chem. Soc.* **1998**, *120*, 8003–8004.
(28) Biros, S. M.; Bergman, R. G.; Raymond, K. N. *J. Am. Chem. Soc.* **2007**, *129*, 12094–12095.
(29) Hastings, C. J.; Pluth, M. D.; Biros, S. M.; Bergman, R. G.; Raymond, K. N. *Tetrahedron* **2008**, *64*, 8362–8367.
(30) Pluth, M. D.; Johnson, D. W.; Szigethy, G.; Davis, A. V.; Teat, S. J.; Oliver, A. G.; Bergman, R. G.; Raymond, K. N. *Inorg. Chem.* **2009**, *48*, 111–120.
(31) Fiedler, D.; Leung, D. H.; Bergman, R. G.; Raymond, K. N. *Acc. Chem. Res.* **2005**, *38*, 349–358.
(32) Pluth, M. D.; Bergman, R. G.; Raymond, K. N. *Acc. Chem. Res.* **2009**, *42*, 1650–1659.
(33) Hastings, C. J.; Pluth, M. D.; Bergman, R. G.; Raymond, K. N. *J. Am. Chem. Soc.* **2010**, *132*, 6938–6940.
(34) Brown, C. J.; Bergman, R. G.; Raymond, K. N. *J. Am. Chem. Soc.* **2009**, *131*, 17530–17531.
(35) For monocationic guests, interior-exterior guest exchange in host **1** is typically much slower than the NMR time scale. For example, the guest exchange rate at room temperature in $D_2O$ solution for $NEt_4^+$ is ~0.006 $s^{-1}$ and ~15 $s^{-1}$ for $NMe_3Bn^+$. This is significantly slower than the time scale for averaging of interior/exterior guest $^1H$ NMR resonances (~1000 $s^{-1}$).
(36) Mugridge, J. S.; Bergman, R. G.; Raymond, K. N. *J. Am. Chem. Soc.* **2010**, *132*, 1182–1183.
(37) Sgarlata, C.; Mugridge, J. S.; Pluth, M. D.; Tiedemann, B. E. F.; Zito, V.; Arena, G.; Raymond, K. N. *J. Am. Chem. Soc.* **2010**, *132*, 1005–1009.
(38) Mugridge, J. S.; Bergman, R. G.; Raymond, K. N. *Angew. Chem., Int. Ed.* **2010**, *49*, 3635–3637.
(39) Leung, D. H.; Bergman, R. G.; Raymond, K. N. *J. Am. Chem. Soc.* **2008**, *130*, 2798–2805.
(40) Davis, A. V.; Fiedler, D.; Seeber, G.; Zahl, A.; van Eldik, R.; Raymond, K. N. *J. Am. Chem. Soc.* **2006**, *128*, 1324–1333.
(41) Davis, A. V.; Raymond, K. N. *J. Am. Chem. Soc.* **2005**, *127*, 7912–7919.
(42) Parac, T. N.; Scherer, M.; Raymond, K. N. *Angew. Chem., Int. Ed.* **2000**, *39*, 1239–1242.
(43) It should be noted that encapsulation within host **1** is responsible for switching the relative ordering of the $CH_2$ and $CH_3$ resonances for $PEt_4^+$. The $^1H$ NMR chemical shifts of $PEt_4^+$ in free $D_2O$ solution (referenced to residual HDO) are as follows: 2.19 ppm ($CH_2$) and 1.21 ppm ($CH_3$).
(44) In $D_2O$, $CD_3OD$, and DMSO-$d_6$, guest **2** is quantitatively encapsulated and its $^1H$ NMR resonances are shifted upfield as would be expected; only in DMF-$d_7$ is the downfield chemical shift observed. This is why DMF is chosen as the as the solvent dielectric for subsequent calculations exploring the chemical shift of $PMe_4^+$ during guest exchange.
(45) Frisch, M. J. et al. *Gaussian 09, Revision A.02*, Gaussian, Inc.: Wallingford CT, 2009.
(46) $^1H$ NMR chemical shifts for the aromatic host protons were not calculated at a higher level of theory both to limit computational cost and because the chemical shifts of these protons are not expected to provide useful structural information. The chemical shifts for the host protons change only slightly upon guest encapsulation (0.0−0.1 ppm) and may also be affected by exterior guest binding.
(47) *OriginPro 8.1*; OriginLab Corporation: Northampton, MA 01060 USA.
(48) The solid-state coordinates could not be used directly. Since X-ray diffraction experiments underestimate C−H bond lengths by ~0.1 Å (see:Churchill, M. W. *Inorg. Chem.* **1973**, *12*, 1213–1214), using these atom coordinates in the GIAO calculations gives $^1H$ NMR chemical shifts that are 2−4 ppm different from experimental values. To solve this problem, the encapsulated guest molecules were minimized (OPLS 2005) with the host atoms frozen, allowing guest C−H bonds to assume more accurate lengths. During these minimizations, the guest conformation and orientation within the host were negligibly altered.
(49) *MacroModel*; Schrodinger: New York, NY, 2010.

(50) Jorgensen, W. L.; Tirado-Rives, J. *Proc. Natl. Acad. Sci. U.S.A.* **2005**, *102*, 6665–6670.
(51) Kleywegt, G. J.; Jones, T. A. *Acta Crystallogr.* **1994**, *D50*, 178–185.
(52) Kleyweget, G. J.; Zou, J. Y.; Kjeldgaard, M.; Jones, T. A. Vol. *F*, pp. 353-356, 366−367.
(53) Molecular mechanics minimization of solid-state host−guest geometries is generally found to expand the volume of the host cavity. It is unknown whether the smaller solid-state cavity volumes, or the expanded mechanics-minimized volumes, correspond most closely to solution-state cavity volumes. However, the NMR shift calculations appear to be relatively insensitive to cavity volume and depend much more strongly on guest orientation and geometry.
(54) Mugridge, J. S.; Szigethy, G.; Bergman, R. G.; Raymond, K. N. *J. Am. Chem. Soc.* **2010**, *132*, 16256–16264.